

Malignant melanoma and lymph node metastases appearing as hyperattenuating masses on computed tomography in a dog

Luzanne van der Laan  | Christelle Le Roux

Department of Companion Animal
Clinical Studies, University of Pretoria,
Onderstepoort, South Africa

Correspondence

Christelle Le Roux, Department of Companion
Animal Clinical Studies, University of Pretoria,
Private Bag X04, Onderstepoort 0110, South
Africa.

Email: christelle.leroux@up.ac.za

Abstract

A 16-year-old male castrated Dachshund cross dog was referred for a dental and a mass on the right side of the face. CT revealed several heterogenous precontrast hyperattenuating masses within the subcutaneous tissue over the masseter muscle, demonstrating marked contrast uptake. The ipsilateral mandibular lymph nodes were mildly enlarged and markedly hyperattenuating on precontrast images. A histopathological final diagnosis of malignant melanoma with regional lymph node metastasis was made, and the hyperattenuating appearance was postulated to be due to its melanin content. This is the first published report of melanoma appearing as hyperattenuating masses on CT in small animals.

KEYWORDS

attenuating, canine, tumor

1 | SIGNALMENT, HISTORY, AND CLINICAL FINDINGS

A 16-year-old male castrated Dachshund cross dog was referred for a dental and a mass on the right side of the face. Eight months prior, the patient had a right-sided lower eyelid mass removed, which affected half the eyelid. A histopathologically diagnosed conjunctival melanocytic neoplasm at the mucocutaneous junction was excised with narrow margins. Due to the highly pigmented appearance, further bleaching and immunohistochemical staining were recommended to determine its biological behavior, but the owner declined them. The patient was on chronic Pimobendan (Vetmedin, Boehringer Ingelheim) at the time of presentation for the treatment of myxomatous mitral valve disease. Clinical examination revealed mild periodontitis with a large, well-circumscribed, lobulated, firm mass at the right mandible and cheek, and a mildly enlarged right-sided mandibular lymph node. Cardiac auscultation revealed a previously confirmed grade four out of six parasternal systolic murmurs, and the rest of the clinical parameters were within normal limits. Blood smear and routine

serum biochemistry were performed, and the only abnormality was a markedly elevated alkaline phosphatase of 1746 U/L (23–212 U/L). Following clinical examination, fine needle aspirates of the mass and right mandibular lymph node were performed, and a provisional diagnosis of melanoma with regional lymph node metastasis was made based on the cytology findings.

2 | IMAGING DIAGNOSIS AND OUTCOME

Three weeks later, a sternal recumbent CT study of the head, chest, and abdomen was performed under general anesthesia for surgical planning as well as metastases screening. A 16 Slice Helical CT scanner (Somatom go.Now, Siemens Healthineers) was used, and the technique settings were as follows for the head: kVP 110, mAs 71, pitch 0.7, slice thickness 1 mm, image matrix 512 × 512, and a rotation time of 1 s. The initial acquisition for the precontrast images was 1 mm transverse slices of the head obtained in a bone (WL 450, WW 1500) and soft tissue (WL 40, WW 400) algorithm. This was followed by

This is an open access article under the terms of the [Creative Commons Attribution](https://creativecommons.org/licenses/by/4.0/) License, which permits use, distribution and reproduction in any medium, provided the original work is properly cited.

© 2024 The Authors. *Veterinary Radiology & Ultrasound* published by Wiley Periodicals LLC on behalf of American College of Veterinary Radiology.

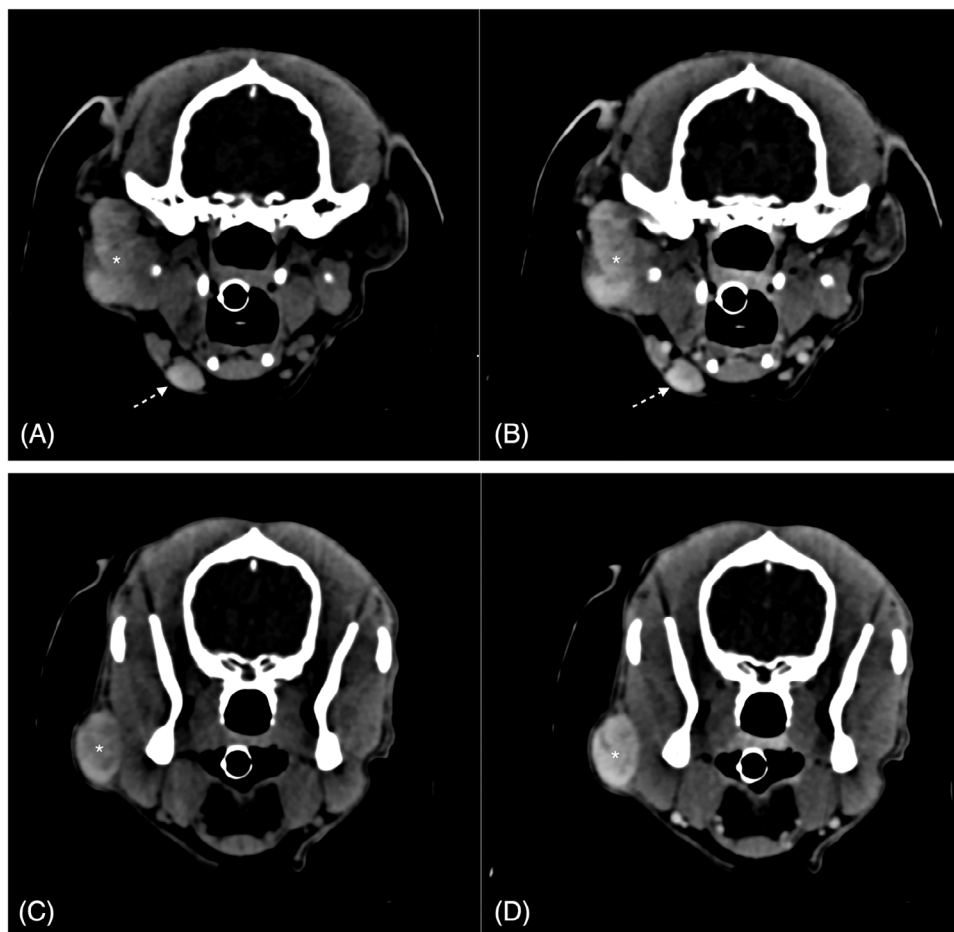


FIGURE 1 Transverse CT images of the head in a soft tissue window (WL 145, WW 241, windowed manually), from caudal (A, B) to rostral (C, D). A and C are precontrast, and B and D are postcontrast images, at the same levels as images A and C, respectively. A and B, The mass (asterisk) is a large lobulated precontrast hyperattenuating mass (160 HU) with marked postcontrast enhancement (192 HU) with central regions of noncontrast enhancement on the right side of the face lateral to the digastric muscle. The enlarged right-sided medial mandibular lymph nodes (arrow) were markedly hyperattenuating precontrast (165 HU precontrast, 192 HU postcontrast). C and D, The rostral most aspect of the precontrast hyperattenuating mass (144 HU mean) (asterisk), demonstrating marked postcontrast enhancement (190 HU) and central regions of noncontrast enhancement on the right side of the face lateral to the masseter muscle.

postcontrast image acquisition of the head, abdomen, and thorax in a bone (head), soft tissue (head, abdomen, and thorax), and lung (thorax: WL -700, WW 1500) algorithm. For the postcontrast image acquisition, the patient was given 2 mL/kg intravenous nonionic iodinated contrast medium (Omnipaque 300 mg/mL, Iohexal GE Healthcare) with hand injection, and transverse images were obtained one minute later. Multiplanar reconstruction and windowing were performed as needed for optimal evaluation of each area of interest.

Immediately rostral to the right parotid salivary gland was a row of several heterogenous precontrast hyperattenuating (compared to the masseter muscle) confluent masses with a mean Hounsfield unit (HU) of 160. They demonstrated marked contrast uptake with several small central regions of noncontrast enhancement due to cavitation or necrosis (Figures 1 and 2). The masses could be seen within the subcutaneous layer, lateral to the rostral most zygomatic arch. The medial margins were in close contact with the masseter muscle and demonstrated no invasion. Rostrally, it was difficult to distinguish from the

soft tissues at the zygomatic arch. Caudally, it was in close contact with the digastric muscle. No bony invasion was noted. Only the right mandibular lymph nodes were mildly enlarged and markedly hyperattenuating on precontrast with a mean HU of 160, similar to the masses. The affected mandibular lymph nodes were more hyperattenuating than when compared with the other lymph nodes. The right medial retropharyngeal lymph node was slightly enlarged with no attenuation changes. No other significant cranial changes were seen in this study.

The right superficial cervical lymph node was moderately enlarged; precontrast attenuation could not be assessed as only postcontrast imaging was available. The thorax was unremarkable except for some unrelated mild bronchial thickening and bronchiectasis, and the abdomen was normal.

Following imaging, multiple biopsies of the masses were taken for histopathology. The sections comprised a neoplasm composed of bundles of polygonal neoplastic cells supported on a collagenous connective tissue stroma. The neoplastic cells had large amounts of darkly

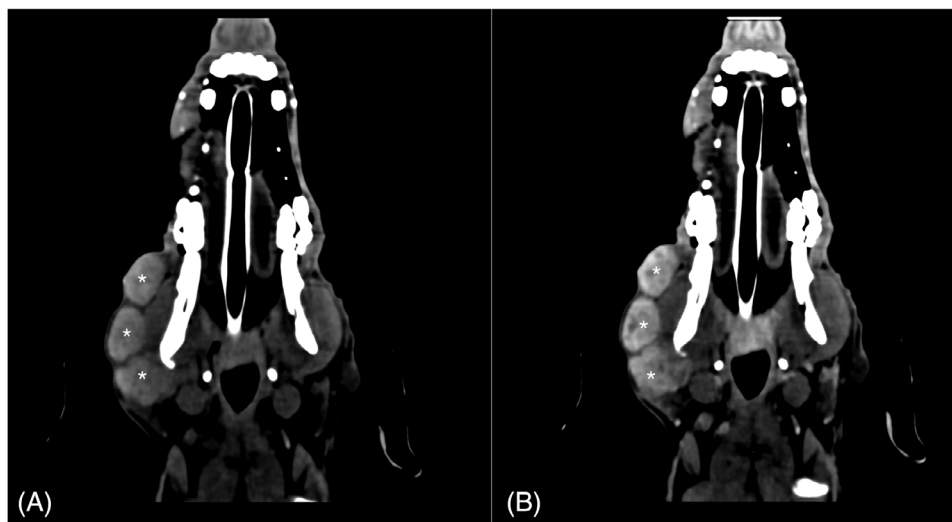


FIGURE 2 Dorsal CT images of the head in a soft tissue window (WL 145, WW 241, windowed manually). A, Precontrast; B, postcontrast. The masses (asterisks) can be seen along the length of the right mandible as three well-defined large precontrast hyperattenuating masses demonstrating marked postcontrast enhancement with central regions of noncontrast enhancement.

pigmented cytoplasm. Based on the histology findings, a diagnosis of malignant melanoma was confirmed, and a final diagnosis of malignant melanoma to the right side of the face with regional lymph node (confirmed on initial cytology), as well as suspected cervical lymph node metastases, was made.

The patient was referred to an internal medicine specialist for further treatment due to the concern that metastasis had already occurred. The patient was subsequently lost to follow-up as they did not present for further treatment.

3 | DISCUSSION

Melanomas are tumors that can affect the skin, digits, oral cavity, eyes, and leptomeninges of dogs, with cutaneous melanomas being the most frequently encountered.¹⁻⁴ The biological behavior of melanoma is extremely diverse and depends on various factors such as size, stage, location, and histological parameters.^{1,2} Melanomas stem from the uncontrolled proliferation of melanocytes. They, therefore, share the same embryonic origin and cellular function. Even though the different subtypes all stem from melanocytes, each subtype has a unique aetiopathogenesis and biological behavior with well-defined landscapes of genetic alterations with different metastatic propensity and local invasiveness.³

Tumor location has been found to be highly predictive of its biological behavior. Cutaneous melanomas have a more benign behavior, and metastasis or reoccurrence after complete excision is rare. Conversely, melanomas of the oral cavity, digits, and mucocutaneous junctions are often associated with a poor prognosis due to high metastatic propensity and local invasiveness.¹⁻⁵ The initial tumor that was diagnosed in this patient was found at the mucocutaneous junction of the eye, and even though not confirmed, its location should have raised suspicion for melanoma with more aggressive biological behavior.

Little information is available on melanin's effect on tissue attenuation in veterinary CT imaging. Only one relevant study to date has been done in equines, and minimal information is available in human medicine. A study done by Dixon et al.⁶ described the CT appearance of histopathologically or cytologically confirmed melanoma in the head of 13 equine patients. They found that all the masses had a similar appearance on CT, with well-defined, predominantly homogenous masses that were hyperattenuating compared to the masseter muscles precontrast (median attenuation of 113.5 HU).⁶ The findings were similar in our case, where lobulated, mostly hyperattenuating precontrast masses were seen.

In small animals, there is currently no information available regarding the effect of melanin on attenuation, and the hyperattenuating appearance of melanoma has also not been previously described. In a recent study by Menghini et al.,⁷ who looked at contrast-enhanced CT predictors of lymph nodal metastasis in 12 dogs diagnosed with oral melanoma with confirmed metastasis and 10 dogs without metastasis as well as 11 melanoma-free dogs, they did not find signs of hyperattenuation on the precontrast CT images. Another recent case report of a dog with oral melanoma described the CT and MRI features, and no hyperattenuation on the precontrast CT images was seen. On MRI, this mass showed a mixture of hyperintense and isointense regions on T1-weighted images, which corresponded to hypointense regions on the T2-weighted images.⁴

In human medicine, the hyperattenuating appearance of melanoma on CT was previously thought to be mainly associated with intratumoral hemorrhage. However, more recently, the changes have been found to be due to a combination of varying degrees of melanin and hemorrhage, with 50% of melanoma cases having the propensity to hemorrhage.^{6,8,9,10,11} The normal HU for fresh hemorrhage or a hematoma is between 65 and 95.¹² Hemorrhage on a CT scan often has a hyperattenuating appearance due to the high degree of cellularity and consequent formation of hematoma breakdown products, and

it was therefore considered an important differential in this case as well.^{13,14}

A human case report of nonhemorrhagic metastatic intracerebral melanoma revealed a hyperattenuating mass on CT and hyperintense mass both on T1 and T2-weighted MR images. Histological examination, in this case, showed typical melanoma with no intratumoral hemorrhage or blood degradation products. They concluded that melanin played a significant role in the increased attenuation seen on CT and the high signal intensity seen on the MR images.¹⁵ Another study by Kukita et al.¹⁶ looked at human patients who were diagnosed with nonhemorrhagic melanotic melanoma, and they also found hyperattenuating lesions on CT, and they attributed this to the melanin content.

A CT review of intracranial melanoma metastases of 98 human patients revealed that 85% of the lesions were hyperattenuating relative to the brain parenchyma.¹⁷ In contrast, muscle metastases most often were soft tissue attenuating on precontrast with only postcontrast enhancement.⁹ On human MRI, it has been shown that melanin results in decreased T1 relaxation time and, when present in sufficient quantities, can result in T1-weighted hyperintensity, which is uncommon in other malignancies but can also be seen with fat and hemorrhage. Melanotic lesions also have a reduced T2-weighted signal, resulting in an appearance similar to that of blood products.^{9,18}

The study done in equines by Dixon et al.⁶ found that significant hemorrhage was rarely seen on histopathology in their cases, and they concluded that the absence of intratumoral hemorrhage proposes that the hyperattenuating appearance directly reflects the melanin content.

Melanin exhibits free radical scavenger properties and has been shown to have a high affinity to bind metal ions such as copper, iron, zinc, and manganese. Copper is required for tyrosinase activity, which is needed during melanin pigment formation and may, during this process, become incorporated into the molecule. It has also been shown by Enochs et al.¹⁹ that melanin has a paramagnetic effect when placed in an external magnetic field, for example, an MRI machine, and it has been proposed that the paramagnetic effects are a result of the metal ion's high binding affinity.^{4,15} The relatively high atomic number of these metal ions could explain the relatively high attenuation of melanomas on CT images.⁶

Apart from hemorrhage, other important differentials to consider in the case of hyperattenuating musculoskeletal masses include tumors that contain mineral content, such as osteoma, osteosarcomas, and ossifying fibroma, but these often also have other distinguishing imaging features not consistent with our findings.⁶

Based on the histopathology findings, the melanoma, in this case, did contain melanin without significant hemorrhage, and based on a combination of the above-mentioned research, the melanin is therefore postulated to have been the reason for the hyperattenuating nature of the masses on the precontrast CT images. The ipsilateral mandibular lymph nodes were mildly enlarged and hyperattenuating precontrast; this was, therefore, also believed to be due to metastases from the melanin-containing masses to this lymph node, as seen on the lymph node aspirates. Only tissue biopsies were performed for histopathology and not complete surgical resection. Therefore,

it cannot be completely excluded that there was no hemorrhage in some areas that were not biopsied. However, due to the high level of Hounsfield units of the masses on the precontrast images, it is believed to be unlikely that hemorrhage played a major role.

In conclusion, these CT findings suggest that malignant melanocytic melanomas can present as precontrast hyperattenuating masses on CT, which may be used to narrow down differential diagnoses of soft tissue masses before sampling and enlarged precontrast hyperattenuating lymph nodes may, in these specific cases, indicate metastases of the melanoma. Based on an extensive literature review, this is the first published report of malignant melanoma appearing as hyperattenuating masses with hyperattenuating regional lymph node metastasis in small animals.

LIST OF AUTHOR CONTRIBUTIONS

Category 1

- (a) Conception and design: van der Laan, Le Roux
- (b) Acquisition of data: van der Laan, Le Roux
- (c) Analysis and interpretation of data: van der Laan, Le Roux

Category 2

- (a) Drafting the article: van der Laan, Le Roux
- (b) Reviewing article for intellectual content: van der Laan, Le Roux

Category 3

- (a) Final approval of the completed article: van der Laan, Le Roux

Category 4

- (a) Agreement to be accountable for all aspects of the work in ensuring that questions related to the accuracy or integrity of any part of the work are appropriately investigated and resolved: van der Laan, Le Roux

ACKNOWLEDGEMENTS

The authors acknowledge the veterinary staff at Valley Farm Animal Hospital for the image acquisition.

CONFLICT OF INTEREST STATEMENT

The authors declare no conflict of interest.

DATA AVAILABILITY STATEMENT

The data used in this study are available from the corresponding author upon reasonable request.

PREVIOUS PRESENTATION OR PUBLICATION

DISCLOSURE

None.

REPORTING CHECKLIST DISCLOSURE

None.

ORCID

Luzanne van der Laan  <https://orcid.org/0009-0002-9077-0705>

REFERENCES

1. Harvey HJ, Macewen EG, Braun D, Patnaik AK, Withrow SJ, Jongeward S. Prognostic criteria for dogs with oral melanoma. *J Am Vet Med Assoc*. 1981; 178:580-582.
2. Spangler WL, Kass PH. The histologic and epidemiologic bases for prognostic considerations in canine melanocytic neoplasia. *Vet Pathol*. 2006; 43(2):136-149.
3. Van Der Weyden L, Brenn T, Patton EE, Wood GA, Adams DJ. Spontaneously occurring melanoma in animals and their relevance to human melanoma. *J Pathol Clin Res*. 2020; 252(1):4-21.
4. Lee A, Lee S, Choi H, Lee Y. Computed tomographic and magnetic resonance imaging features of oral melanoma in a dog. *J Vet Clin*. 2023; 40(6):370-374.
5. Bolon B, Calderwood Mays MB, Hall BJ. Characteristics of canine melanomas and comparison of histology and DNA ploidy to their biologic behavior. *Vet Pathol*. 1990; 27(2):96-102.
6. Dixon J, Smith K, Perkins J, Sherlock C, Mair T, Weller R. Computed tomographic appearance of melanomas in the equine head: 13 cases. *Vet Radiol Ultrasound*. 2016; 57(3):246-252.
7. Menghini TL, Schwarz T, Dancer S, Gray C, Macgillivray T, Bowlit Blacklock KL. Contrast-enhanced CT predictors of lymph nodal metastasis in dogs with oral melanoma. *Vet Radiol Ultrasound*. 2023; 64(4):694-705.
8. Ginaldi S, Wallace S, Shalen P, Luna M, Handel S. Cranial computed tomography of malignant melanoma. *AJR Am J Roentgenol*. 1981; 136:145-149.
9. Patnana M, Bronstein Y, Szklaruk J, et al. Multimethod imaging, staging, and spectrum of manifestations of metastatic melanoma. *Clin Radiol*. 2011; 66:224-236.
10. Wong VK, Lubner MG, Menias CO, et al. Clinical and imaging features of noncutaneous melanoma. *AJR Am J Rounetgenol*. 2017; 208(5):943-959.
11. Kondziolka D, Bernstein M, Resch L, et al. Significance of hemorrhage into brain tumors: clinicopathological study. *J Neurosurg*. 1987; 67(6):852-857.
12. Kamalian S, Lev MH, Gupta R. computed tomography imaging and angiography- principles. *Handb Clin Neurol*. 2016; 135:3-20.
13. William G. Bradley MRI of intracranial hemorrhage. *Contemp Diagn Radiol*. 2016; 39:1-6.
14. Parizel P, Makkat S, Van Miert E, Van Goethem J, Van Den Hauwe L, De Schepper A. Intracranial hemorrhage: principles of CT and MRI Interpretation. *Eur Radiol*. 2001; 11(9):1770-1783.
15. Uozumi A, Saegusa T, Ohsato K, Yamaura A. Computed tomography and magnetic resonance imaging of nonhemorrhagic, metastatic melanoma of the brain- case report. *Neurol Med Chir*. 1990; 30(2):143-146.
16. Kukita C, Nose T, Nakagawa K, et al. Characteristic findings of computed tomography in cerebral metastatic melanomas. *CT Kenkyu*. 1986; 8:195-201.
17. Mcgann GM, Platts A. Computed tomography of cranial metastatic malignant melanoma: features, early detection and unusual cases. *Br J Radiol*. 1991; 64(760):310-313.
18. Escott EJ. A variety of appearances of malignant melanoma in the head: a review. *Radiographics*. 2001; 21(3):625-639.
19. Enochs WS, Petherick P, Bogdanova A, Mohr U, Weissleder R. Paramagnetic metal scavenging by melanin: MR imaging. *Radiology*. 1997; 204(2):417-423.

How to cite this article: van der Laan L, Le Roux C. Malignant melanoma and lymph node metastases appearing as hyperattenuating masses on computed tomography in a dog. *Vet Radiol Ultrasound*. 2024;65:339-343. <https://doi.org/10.1111/vru.13366>